



Published in final edited form as:

*Clin Cancer Res.* 2017 January 15; 23(2): 441–453. doi:10.1158/1078-0432.CCR-16-0492.

## FOLLICLE-STIMULATING HORMONE RECEPTOR IS EXPRESSED BY MOST OVARIAN CANCER SUBTYPES AND IS A SAFE AND EFFECTIVE IMMUNOTHERAPEUTIC TARGET

Alfredo Perales-Puchalt<sup>a</sup>, Nikolaos Svoronos<sup>a</sup>, Melanie R Rutkowski<sup>a</sup>, Michael J Allegrezza<sup>a</sup>, Amelia J Tesone<sup>a</sup>, Kyle K Payne<sup>a</sup>, Jayamanna Wickramasinghe<sup>b</sup>, Jenny M Nguyen<sup>a</sup>, Shane W O'Brien<sup>c</sup>, Kiranmai Gumireddy<sup>a</sup>, Qihong Huang<sup>a</sup>, Mark G. Cadungog<sup>d</sup>, Denise C Connolly<sup>c</sup>, Julia Tchou<sup>e</sup>, Tyler J Curie<sup>f</sup>, and Jose R. Conejo-Garcia<sup>a</sup>

<sup>a</sup>Tumor Microenvironment and Metastasis Program, The Wistar Institute, Philadelphia, PA 19104, USA.

<sup>b</sup>Center for Systems and Computational Biology, The Wistar Institute, Philadelphia, PA 19104, USA.

<sup>c</sup>Molecular Therapeutics Program, Fox Chase Cancer Center, 333 Cottman Avenue, W310, Philadelphia, PA 19111.

<sup>d</sup>Helen F. Graham Cancer Center, Christiana Care Health System, 4701 Ogletown-Stanton Road, Newark, DE 19713, USA.

<sup>e</sup>Division of Endocrine and Oncologic Surgery, Department of Surgery, University of Pennsylvania, Philadelphia, PA 19104-1693, USA.

<sup>f</sup>Department of Medicine, University of Texas Health Science Center at San Antonio, San Antonio, TX 78229, USA.

### Abstract

**Purpose**—Define the safety and effectiveness of T-cells re-directed against Follicle-Stimulating Hormone Receptor (FSHR)-expressing ovarian cancer cells.

**Experimental Design**—FSHR expression was determined by Western-blot, immunohistochemistry and Q-PCR in 77 human ovarian cancer specimens from 6 different histological subtypes and 20 human healthy tissues. The effectiveness of human T-cells targeted with full-length FSH *in vivo* was determined against a panel of patient-derived xenografts. Safety and effectiveness were confirmed in immunocompetent tumor-bearing mice, using constructs targeting murine FSHR and syngeneic T-cells.

**Results**—FSHR is expressed in gynecologic malignancies of different histological types, but not in non-ovarian healthy tissues. Accordingly, T-cells expressing full-length FSHR-re-directed chimeric receptors mediate significant therapeutic effects (including tumor rejection) against a panel of patient-derived tumors *in vivo*. In immunocompetent mice growing syngeneic, orthotopic,

and aggressive ovarian tumors, fully murine FSHR-targeted T-cells also increased survival without any measurable toxicity. Notably, chimeric receptors enhanced the ability of endogenous tumor-reactive T-cells to abrogate malignant progression upon adoptive transfer into naïve recipients subsequently challenged with the same tumor. Interestingly, FSHR-targeted T-cells persisted as memory lymphocytes without noticeable PD-1-dependent exhaustion during end-stage disease, in the absence of tumor cell immunoeediting. However, exosomes in advanced tumor ascites diverted the effector activity of this and other chimeric receptor-transduced T-cells away from targeted tumor cells.

**Conclusions**—T-cells redirected against FSHR<sup>+</sup> tumor cells with full-length FSH represent a promising therapeutic alternative against a broad range of ovarian malignancies, with negligible toxicity even in the presence of cognate targets in tumor-free ovaries.

### Keywords

Immunotherapy; ovarian cancer; CAR T-cell; tumor immunology; Follicle stimulating hormone receptor

## INTRODUCTION

Epithelial ovarian cancers of different histological types are responsible for the death of >14,000 women each year in the US (1). Despite advances in surgery and chemotherapy, 5-year survival rates have barely changed in the last 40 years. Ovarian cancer is, however, an immunogenic tumor (2-10). Therefore, immunotherapies offer great promise to reverse this dismal prognosis (11, 12).

In recent years, transferring autologous T-cells engineered to express chimeric antigen receptors (CARs) has shown impressive cures for patients with chemo-resistant hematologic malignancies (13-15). However, several hurdles have thus far prevented the success of this technology against solid tumors, including ovarian cancer. The most challenging obstacle in developing CAR therapies is the identification of specific targets expressed on the surface of tumor cells that are not shared with healthy tissues. Identifying such targets is crucial for avoiding potentially deadly side-effects.

The follicle-stimulating hormone receptor (FSHR) is thought to be selectively expressed in women in ovarian granulosa cells (16) and at low levels in the ovarian endothelium (17). Most importantly, this surface antigen is expressed in 50-70% of serous ovarian carcinomas, although its expression in other histological types of ovarian cancer remains unknown (18-25). In addition, recent studies indicate that circulating levels of FSH correlate with worse outcome in ovarian cancer patients (26). Given that oophorectomy is a standard procedure in the treatment of ovarian cancer, targeting the FSHR should not cause damage to healthy tissues. Therefore, FSHR could be an ideal therapeutic target to direct T-cells against ovarian cancer using chimeric receptors.

Preclinical testing of CARs has been done in immunodeficient xenograft-bearing mice, which do not share the targets of chimeric receptors and therefore cannot predict potential, clinically-relevant adverse effects. To understand the interaction between CAR T-cells, the

host immune system, and the endogenous target potentially expressed in healthy tissues, we generated Chimeric Endocrine Receptors (CER) against human FSHR, to exploit receptor-ligand interactions through the expression of full-length human FSH. We also engineered T-cells expressing the murine counterparts of all FSH signaling domains for use in immunocompetent tumor-bearing mice (13). Our results demonstrate that targeting FSHR with T-cells expressing hormone-derived chimeric receptors is safe, specific, effective, and capable of boosting preexisting, endogenous anti-tumor immunity.

## MATERIALS AND METHODS

### Animals and cell lines

Wild-type C57BL/6 and Ly5.1 mice were purchased from National Cancer Institute or from Charles River. NOD-SCID IL2R $\gamma$ <sup>null</sup> (NSG) mice, originally from Jackson labs, were maintained by The Wistar Institute animal facility. Animal experiments were approved by the Institutional Animal Care and Use Committee at The Wistar Institute.

Parental ID8 cells were provided by Katherine Roby (Department of Anatomy and Cell Biology, University of Kansas Medical Center, Kansas City, KS) and retrovirally transduced to express *Defb29* and *Vegf-a* (27) and murine FSHR. We generated ID8-*Defb29/Vegf-a* flank or intraperitoneal tumors as described previously (9). A7C11 is a murine cell line generated from orthotopic p53/KRas-driven mouse breast tumors (28, 29), which was retrovirally transduced to express murine FSHR. Patient-derived xenografts (PDX) FCCC-OV-16, WISTAR-1 and WISTAR-2 were implanted subcutaneously into NSG mice followed by intratumoral T-cell administration; WISTAR-3 was implanted as a tissue fragment under the ovarian bursa in NSG mice and was treated with intraperitoneal administration of T-cells.

We measured flank tumors with calipers and calculated tumor volumes as  $1/2 \times (L \times W \times W)$ , where L is the longer of two dimensions.

OVCAR-3, CaOV3, RNG1, OVTOKO and TOV-21G were provided by Dr. Rugang Zhang (The Wistar Institute).

### Design of chimeric antigen receptors and soluble FSHR

We designed the chimeric antigen receptor constructs using the signal peptide of murine CD8 $\alpha$ , followed by a fusion of the full length murine FSH $\beta$  and CG $\alpha$  peptides linked by a glycine/serine spacer, followed by murine CD8 $\alpha$  hinge and transmembrane domain and an intracellular fragment of murine 4-1BB and CD3 $\zeta$ . We ordered the construct from Genescript flanked by EcoRI and NotI and cloned into pBMN-I-GFP retroviral vector. The corresponding human sequences were ordered to generate the human FSHR-targeted chimeric receptor.

To generate the N-terminal extracellular domain of FSHR we cloned the sequence encoding FSHR from residues 1 to 268 into pBMN-I-GFP retroviral vector and infected 293T cells.

## Human samples

Human ovarian carcinoma tissues were procured under a protocol approved by the Committee for the Protection of Human Subjects at Dartmouth-Hitchcock Medical Center (#17702); and under a protocol approved by the Institutional Review Board at Christiana Care Health System (#32214) and the Institutional Review Board of The Wistar Institute (#21212263). A panel of cDNA samples from healthy human tissues was purchased from Clontech.

Patient-derived xenograft model FCCC-OC-16 was established by direct implantation of human ovarian tumor tissue in immunocompromised mice under Institutional Review Board and Institutional Care and Use Committee approved protocols at Fox Chase Cancer Center.

## Analysis of TCGA data

Aligned Sequence files related to solid ovarian cancer samples were downloaded from TCGA data portal (2015). Downloaded files include whole exon sequencing and outcome data. Scores (number of tags in each transcript) were obtained from each sample, normalized with respect to total tags in the sample as well as total tags in the chromosome, and expressed as FPKM (Fragments/Kb of transcript per million mapped reads).

## Retrovirus production and transduction of T-cells

We generated retrovirus by transfecting Eco-Phoenix cells with pBMN-I-GFP or pBMNI-GFP-FSHCER. Briefly, we plated the Phoenix cells in a 10 cm culture dish. When the cells reached 80-90% confluence we transfected them with a mix of DNA, CaCl<sub>2</sub> and 2X HBSS. We collected the supernatant containing the retroviral particles 48 and 72 hours after transfection and stored them at -80° C.

For mouse T-cell transduction, after red blood cell lysis we resuspended splenocytes at 2×10<sup>6</sup> cells/mL in a 24-well plate with 50 U/mL of IL-2 (Peprotech), 1 µg/mL of IL-7 (Peprotech) and 50 µL/mL of anti-mouse CD3/CD28 beads (Invitrogen). We performed two spin-infections at 18 and 36 hours on Retronectin coated plates (Takara) and magnetically removed the CD3/CD28 beads at day 4 after isolation. We counted the T cell number every 2 days and added RPMI + IL-2 + IL-7 to maintain a concentration of 10<sup>6</sup> cells/mL. At day 7 T-cells were sorted for GFP and used for adoptive cell transfer.

Human peripheral blood lymphocytes were obtained by leukapheresis/elutriation and identically transduced with human reagents.

## Cytotoxicity assay

We plated 10,000 target tumor cells in flat bottom 96 well plate. Before adding T-cells, we washed away the tumor conditioned media and added fresh media with no beta-mercaptoethanol and the appropriate number of T-cells per well (in 200 uL). T-cells were FSHCER or mock transduced. Following 18 hours we collected T-cells and tumor cells by trypsinization and proceeded to flow cytometric analysis of cellular cytotoxicity (30). We stained cells with Annexin V and Zombie Yellow or 7-AAD (Biolegend), and gated out the T-cells by FSC and SSC using a no T-cell control (**Supplemental Figure 1a**). To confirm the

validity of the flow cytometric assay in our hands, we transduced OVCAR-3 tumor cells with a luciferase expressing vector and checked for cytotoxicity using the Luciferase Assay (Promega) (**Supplemental Figure 1b**). Cytotoxicity was calculated as (maximum viability control – individual well)/(maximum viability control – maximum death control)\*100 as a percentage.

### Interferon- $\gamma$ determination

We plated 10,000 ID8-*Defb29/Vegf-a/Fshr* in flat bottom 96 well plate and co-cultured overnight with FSHCER or mock transduced T-cells. We measured interferon- $\gamma$  using ELISA (Biologend) following manufacturer instructions.

For interferon- $\gamma$  ELISPOT (eBioscience) we primed 2 million bone marrow-derived dendritic cells (BMDC) with 200,000 irradiated (100 Gy + 30 minutes UV) ID8-*Defb29/Vegfa/Fshr* cells overnight. The next day we plated 10,000 T cells with 1,000 BMDC and measured the number of spots 72 hours later on an ELISPOT reader using Immunospot software (CTL).

### Flow cytometry

We used a BD LSRII flow cytometer or BD FACSAria cell sorter (BD Biosciences). Anti-mouse antibodies used were directly fluorochrome conjugated. We used: anti-CD3e (17A2), CD4 (RM4-5), CD8b (YTS156.7.7), CD45 (30-F11), CD45.1 (A20), CD45.2 (104), CD44 (IM7), CD69 (H1.2F3), CD62L (MEL-14), PD-1 (29F.1A12) (all from Biologend or Tonbo Biosciences). Live/dead exclusion was done with Zombie Yellow or 7-AAD (Biologend).

### Exosome isolation

Exosomes were isolated from ascites using the Total Exosome Isolation Reagent (Invitrogen) following manufacturer's instructions.

### Immunoblotting

Frozen human ovarian tumor specimens were mechanically disassociated. Protein extraction, denaturation and western blotting were performed as previously described (29). Membranes were blotted with anti-FSHR (FSHR-18, ATCC)(31) and anti- $\beta$ -actin (A5441, Sigma-Aldrich). Images were captured with ImageQuantLAS 4000 (GE Healthcare Life Sciences).

### Immunohistochemistry

Tumor microarrays from paraffin embedded ovarian cancers and paraffin embedded mouse tumors were subjected to antigen retrieval and deparaffinized. Slides were then fixed with acetone and washed with PBS, and sections blocked using normal goat serum followed by staining with FSHR18 antibody (31), followed by a biotinylated goat anti-mouse and completion of immunohistochemical procedure according to manufacturer instructions (Vector Labs). As positive control we used CaOV3 tumors (**Supplemental Figure 2a**). We stained for osteoclasts using Leukocyte Acid Phosphatase TRAP Kit (Sigma-Aldrich). Femurs and tibias were placed in 10% formalin for 24hours, and bone decalcification was performed using 14% EDTA in PBS at 4°C for 7 days. We removed EDTA by rinsing bones

in tap water for 30 minutes and placed bones in 70% ethanol until paraffin embedding and sectioning.

Slides were viewed using Nikon ECLIPSE 80i microscope and the NIS-Element Imaging software.

### Quantitative real-time PCR

Tissue RNA was isolated from snap-frozen samples by mechanical disruption and extracted using RNeasy kits (QIAGEN) according to manufacturer's instruction. RNA was reverse transcribed using High Capacity Reverse Transcription kits (Applied-Biosystems). Quantification of human FSHR was performed on the 7500 Fast Real Time PCR system (Applied Biosystem) using Taqman assay reagents and primers (Forward: 5'-ATGGAAGCCAGCCTCACCTAT-3'; and Reverse: 5'-TCTGACCCCTAGCCTGAGTCATA-3'), and TaqMan probe 5'-FAM/ACGGCAAAT/ZEN/CTCTGAGCTTCATCCA-IBFQ-3'. Expression was normalized by GAPDH levels (Assay ID: Hs99999905). Quantification of mouse FSHR was performed using SYBR green reagents and primers (Forward: 5'-TTTTCTGGATTTGGGGACCT-3'; and Reverse: 5'-ATGCAAGTTGGGTAGGTTGG-3'). mRNA expression was normalized by GAPDH levels (primers Forward: 5'-CCTGCACCACCAACTGCTTA-3'; and Reverse: 5'-AGTGATGGCATGGACTGTGGT-3'). The average of three independent analyses for gene and sample was calculated using the threshold cycle (Ct) method and was normalized to the endogenous reference control gene GAPDH.

### Biochemical determinations

AST, ALT, glucose and creatinine were determined by the Mouse Phenotyping, Physiology and Metabolism Core (University of Pennsylvania) using Catalyst Dx Chemistry Analyzer (Idexx Laboratories).

IL-6 was measured in plasma using an IL-6 ELISA Kit (Biolegend) following manufacturer's instructions.

### Statistical analysis

Unless noted otherwise, all experiments were repeated at least twice and with similar results. Differences between the means of experimental groups were calculated using a two-tailed unpaired Student's *t* test or two-way ANOVA with Bonferroni correction where two categorical variables were measured. Error bars represent standard error of the mean. Survival rates were compared using the log-rank test. All statistical analyses were done using Graph Pad Prism 5.0.  $p < 0.05$  was considered statistically significant.

## RESULTS

### FSHR is expressed in aggressive ovarian carcinomas of multiple histological subtypes

To understand the relevance of FSHR as an immunotherapeutic target in human ovarian cancer of different histological types, we first analyzed TCGA datasets from 404 high-grade serous ovarian carcinomas, which represent ~70% of all epithelial ovarian cancers (EOC)

(32). We found that 56.4% of these tumors express FSHR mRNA (**Figure 1a**). In addition, 4.7% of 1,095 breast carcinomas in TCGA datasets also expressed FSHR (**Figure 1b**), suggesting that FSHR targeting could also be effective in other malignancies. Widespread expression of FSHR was confirmed in Western blot and immunohistochemical analysis of 28 stage III/IV serous ovarian carcinomas from our tumor bank, with 50% of the tumors analyzed expressing FSHR (**Figure 1c**), consistent with previous studies (18-25). Characterization of the expression of FSHR in other histological subtypes identified positive protein signal in 70% of endometrioid carcinomas (~10% of EOC; 23 tumors analyzed), 67% of mucinous ovarian carcinomas (~3% of EOC; 9 tumors analyzed) and 33% of clear cell ovarian carcinomas (~10% of EOC; 12 tumors analyzed), but not in ovarian carcinosarcomas (**Figure 1d-f**; 4 tumors analyzed). In addition, we found FSHR expression in 3/3 clear cell ovarian cell lines (RNG1, TOV-21G and OVTOKO; **Figure 1g**) but expression was not detected in a granulosa cell tumor specimen (**Figure 1e**). A good correlation was observed between protein and mRNA levels (**Supplemental Figure 2b**). Therefore, besides expression in most serous carcinomas, FSHR expression could open new treatment opportunities for poor prognosis subtypes, such as mucinous and clear cell, for which there are currently few effective therapies (33).

### **FSHR can be effectively targeted to treat patient-derived ovarian cancer through the use of chimeric receptors**

To target the FSHR by redirecting T-cells, we generated a human chimeric receptor using the full-length of the two subunits of the human FSH hormone, linked by a glycine/serine spacer, in frame with a transmembrane domain, the intracellular domain of co-stimulatory 4-1BB, and CD3 $\zeta$  (FSHCER; **Figure 2a**). As expected, FSHCER expressing T-cells killed cultured OVCAR-3 target cells, a well-defined positive control (22, 34), in dose-dependent manner, compared to mock transduced T-cells and without killing FSHR<sup>-</sup> K562 cells (**Figure 2b**). In addition, FSHCER T-cells abrogated the growth of xenografted FSHR<sup>+</sup> CaOV3 ovarian cells in immunodeficient mice, while mock-transduced T-cells allowed accelerated tumor progression (**Figure 2c**).

To understand the immunotherapeutic potential of targeting FSHR in heterogeneous ovarian malignancies expressing variable target levels, we next treated pairs of NSG mice growing identically established FSHR<sup>+</sup> ovarian patient-derived xenograft (PDX) tumors with FSHCER T-cells (case mouse) or mock transduced T-cells (control paired mouse with the same xenograft). Remarkably, FSHCER T-cells induced rejection of the human ovarian PDX model expressing the highest levels of FSHR (PDXFCCC-OC-16), and delayed the growth of a second model (Wistar-1) with FSHR levels lower than most primary ovarian malignancies (**Figure 2d&e**, and **Supplemental Figure 2c**). In both cases, administration of mock transduced T-cells into paired mice growing the same PDX tumor allowed for steady tumor growth (**Figure 2d&e**). Anti-tumor effects, however, appear to depend on FSHR expression levels, as no changes were observed against a third PDX model with lower FSHR expression (Wistar-2; **Figure 2d&e**).

To confirm that allogeneic recognition of tumors by heterologous T-cells is not required for FSHCER activity and to confirm effectiveness at the orthotopic location, we treated another

pair of mice growing a different FSHR<sup>+</sup> PDX (Wistar 3) in the ovarian bursa with (autologous) T-cells from the peripheral blood of the same patient. As shown in **Figure 2f**, a solid tumor mass grew in the mouse treated with mock transduced T-cells, while the tumor growing in the mouse receiving FSHRCER T-cells exhibited massive central necrosis and only retained tumor tissue at the margins. Taken together, these results support that chimeric receptors using entire subunits of the FSH hormone can effectively redirect the cytotoxic activity of T-cells against a variety of patient-derived FSHR<sup>+</sup> ovarian carcinomas.

### **Chimeric receptor-expressing T-cells are safe and effective against different established tumors in immunocompetent mice**

An important concern regarding the use of chimeric receptor-targeted immunotherapies is the occurrence of off-tumor effects. Further supporting the therapeutic potential of FSHRCER T-cells, we confirmed that only tumor-free ovaries, and not any other healthy human tissues tested, expressed FSHR at the mRNA level (**Figure 3a**). Of note, this includes liver tissue, where a recent report has suggested possible expression of FSHR in tissue surrounding a hepatocellular carcinoma (35).

To rule out potential *in vivo* toxicity due to unknown FSHR expression in any healthy tissue, we then generated a mouse FSHCER construct with the murine counterparts of all domains expressed in human T-cells. As expected, ID8-*Defb29/Vegf-a* tumor cells, an aggressive ovarian cancer model engineered to accelerate peritoneal carcinomatosis and ascites *in vivo* (4, 8, 10, 36), elicited robust secretion of IFN- $\gamma$  by FSHCER mouse T-cells upon ectopic expression of FSHR, to a much greater extent than in the absence of ectopic FSHR expression (**Figure 3b**). FSHCER-specific T cell responses were consistent when CD4 and CD8 T-cells were independently stimulated (**Figure 3c**) and, as with their human counterparts, mouse FSHCER T-cells specifically killed FSHR-expressing tumor cells in a dose dependent manner (**Figure 3d**). Accordingly, only two intraperitoneal injections of  $1-1.5 \times 10^6$  FSHCER T-cells were sufficient to significantly prolong survival in this aggressive orthotopic model (4, 8, 10, 27, 36-38), compared to mock-transduced T-cells, in multiple independent experiments (*e.g.*, **Figure 3e**). This supports the NCI recommendation for an intraperitoneal treatment of this disease, because under the same conditions, intravenous administration of FSHCER T-cells was unable to delay ovarian tumor progression (**Figure 3f**). As expected, treatment of untransduced parental ID8-*Defb29/Vegf-a* tumors resulted in no survival benefit (**Figure 3g**).

Equally important, no obvious adverse effects were observed in these experiments. To identify potential deleterious consequences of targeting the expression of FSHR in any unknown healthy tissues which could lead to on-target, off-tumor unacceptable side effects, we analyzed weight, obvious phenotypic changes and general organ biochemistry to screen for potential organic failures. There was no evidence of weight loss or any signs of distress throughout the treatment (not shown). Levels of (AST/ALT) liver enzymes, creatinine or glucose in the serum of FSHCER T-cell-treated mice remained unchanged, compared to control mice injected with PBS (**Figure 3h**). We found, however, a significant increase in serum IL-6 in FSHCER T-cell-treated mice, which also occurred in mice receiving mock-transduced T cells (**Figure 3h**). This recapitulates cytokine patterns previously observed in



CAR T-cell-treated patients (39). Because FSHR signaling has been also suggested in osteoclasts, we also ruled-out any obvious alterations in bone density or the frequency of osteoclasts in FSHCER-treated versus untreated mice (not shown).

Because we also identified mRNA expression of FSHR in 4.7% of TCGA breast carcinomas, and because FSHR could be expressed in certain metastatic lesions (40), we treated mice with FSHR-transduced breast tumors generated with orthotopic p53/KRas-driven malignant cells (28, 38). As shown in **Figure 3i**, systemic administration of FSHRCER T-cells significantly delayed the progression of established tumors, compared to the administration of mock-transduced lymphocytes. Again, no obvious toxicity was detected at any level.

Overall, these results demonstrate that T-cells re-directed against murine ovarian or breast cancer cells overexpressing FSHR with hormone-targeted chimeric receptors induce significant therapeutic benefits in immunocompetent mice with different established, aggressive tumors, without detectable toxicity or alternative targeting of any healthy tissue.

### **Chimeric receptor-expressing T-cells boost pre-existing, endogenous T-cell-dependent anti-tumor immunity**

To understand the relative contribution of different T-cell subsets to the reproducible anti-tumor activity of FSHCER lymphocytes, we next treated different cohorts of ID8-*Defb29/Vegf-a* tumor-bearing mice with either FSHCER-transduced CD4 or CD8 T-cells, alone or in combination. Interestingly, CD4 T-cells expressing chimeric receptors were as effective as a mix of unsegregated lymphocytes, while CD8 T-cells alone were less effective, although better than mock-transduced T-cells (**Figure 4a**).

We then took advantage of our immunocompetent mouse model to dissect the interaction of adoptively transferred CER T-cells with an intact immune system, which is incompletely understood and impossible to dissect in immunodeficient mice. We hypothesized that the specific cytotoxic activity of FSHCER T-cells should result in antigen spreading and decreased immunosuppressive burden, which could have a significant effect on pre-existing anti-tumor immunity. To test this proposition, we treated different cohorts of CD45.2<sup>+</sup> mice bearing orthotopic FSHR<sup>+</sup> ID8-*Defb29/Vegf-a* syngeneic tumors with either congenic CD45.1<sup>+</sup> FSHCER T-cells, mock-transduced T-cells or vehicle (PBS). Pre-existing T-cells of host origin (CD45.2<sup>+</sup>, to differentiate them from transferred FSHCER T-cells) were sorted from the peritoneal cavity 1-2 weeks after treatment and subjected to IFN- $\gamma$  ELISPOT analysis (**Figure 4b**). The frequency of endogenous IFN- $\gamma$ -producing T-cells responding to dendritic cells pulsed with double (UV +  $\gamma$ )-irradiated ID8-*Defb29/Vegf-a/Fshr* tumor cells was dramatically higher in mice treated with FSHCER T-cells compared to endogenous T-cells from both the mock-transduced and vehicle treated groups (**Figure 4c**). Most importantly, endogenous T-cell responses were also capable of reducing malignant progression, because adoptive transfer of host-derived (CD45.2<sup>+</sup>) splenic T-cell from mice treated with FSHCER T-cells (CD45.1<sup>+</sup>) into naïve, syngeneic mice resulted in significantly smaller tumors upon re-challenge with the same ID8-*Defb29/Vegf-a* cells, compared to the effect of T-cells from control tumor-bearing mice (**Figure 4d&e**).

Together, our results indicate that CD4 T-cells are major contributors to consistent therapeutic benefits, and that the overall cytotoxic activity of T-cells re-directed against tumor cells with chimeric receptors boosts the activity of endogenous T-cells. This response should be able to delay malignant progression regardless of whether tumors lose targeted antigens through immunoediting.

### **Chimeric receptor-expressing T-cells persist in the absence of immunoediting, but are diverted from tumor beds by tumor ascites**

Our results indicate that hormone-targeted T-cells are both safe and effective against established aggressive malignancies. To understand tumor-induced mechanisms that could limit the effectiveness of chimeric receptor-expressing T-cells *in vivo*, we next tested whether tumor cells could lose the targeted surface molecules through immunoediting. Notably, fresh FSHCER T-cells reacted equally strongly by secreting IFN- $\gamma$  in response to FSHR-transduced tumor cells sorted from the peritoneal cavity of mice previously treated with FSHCER- or mock-transduced T-cells, or PBS (**Figure 5a&Supplemental Figure 3**), indicating persistence of targeted FSHR.

Another possibility is that chimeric receptor-targeted T-cells do not persist in cancer-bearing hosts. We therefore again took advantage of the congenic marker CD45.1 expressed in FSHRCER T-cells and sacrificed FSHR-expressing ID8-*Defb29/Vegf-a* tumor-bearing mice at days 5, 10 and 15 after intraperitoneal administration of FSHCERT-cells. Five days after T-cell administration, we saw a peak of FSHCER T-cells in the peritoneal cavity, with similar proportions of CD8 *versus* CD4 lymphocytes (**Figure 5b&c**). Both subsets were activated (CD44<sup>+</sup>CD69<sup>+</sup>) in tumor (peritoneal) beds at this early stage (45.5% and 3.1%, respectively) (**Figure 5d**). However, proportions and absolute numbers (not shown) of transferred T-cells decreased on days 10 and 15, accompanied by a higher percentage of CD4 T-cells relative to CD8, and retention of activation markers (**Figure 5b-d**). In both spleen and tumor draining lymph nodes, we observed a peak of accumulation at day 10, with trafficking as early as day 5. These T-cells are mostly CD4<sup>+</sup> (90.5%) with a central memory phenotype (CD44<sup>+</sup>CD62L<sup>+</sup>) (**Figure 5e**) and represented 0.8% of total T-cells. At terminal stages of malignant progression, FSHCER T-cells were still clearly and reproducibly detectable in the spleen (0.6% of total T-cells) (**Figure 5f**). T-cell detection in solid tumors was unreliable for technical reasons and could not be assessed. Surprisingly, no FSHCER T-cells could be detected at this stage in tumor ascites. This cannot be attributed to classical T-cell exhaustion, because only a minority of T-cells (8% in CD8 and 31% in CD4) expressed PD-1 on the cell surface (**Figure 6a**).

The ID8-*Defb29/Vegf-a* tumor system quickly generates massive ascites. To determine whether immunosuppressive factors in tumor ascites could induce T-cell death, we then co-incubated FSHR-expressing ID8-*Defb29/Vegf-a* tumor cells and targeted FSHCER T-cells in the presence of increasing amounts of tumor-derived ascitic fluid. Unexpectedly, filtered (cell-free) tumor ascites increased the reactivity (IFN- $\gamma$  secretion) of FSHCER T-cells in a dose-dependent manner (**Figure 6b**). This was the result of recognition of FHSR of tumor cell origin in ascites because identically treated mock-transduced T-cells did not react against FSHR<sup>+</sup> tumor cells in the presence of ascites. Similar activation of CER T-cells was

observed in transwell experiments where tumor cells were physically separated from FSHCER T-cells (**Figure 6c**), and was recapitulated by incubation with fresh ascites from ID8-*Defb29/Vegf-a/Fshr* bearing mice (**Figure 6d**), but not plasma from a tumor-free mouse (**Figure 6e**). However, incubation with supernatants from cells transduced with a soluble form containing the N-terminal extracellular domain of FSHR was not sufficient to elicit FSHCER T-cell activation (**Figure 6e**). We therefore hypothesized that a membrane-bound form of FSHR contained in exosomes from the tumor cells could be responsible for activating FSHCER T-cells. Supporting this proposition, exosomes isolated from the ascites of ID8-*Defb29/Vegf-a/Fshr* bearing mice specifically activated FSH CERT cells (but not mock-transduced T cells) upon co-incubation (**Figure 6e**).

Finally, to define whether soluble or exosome-contained forms of additional targets could impair the effectiveness of other CAR T cell formulations, we transduced T-cells with a CAR bearing the anti-mesothelin SS scFv (GenBank: AF035617.1) being used in clinical trials (41). As shown in **Figure 6f**, incubation with human ascites from an ovarian cancer patient was sufficient to elicit a dramatic IFN- $\gamma$  response in anti-mesothelin CAR T cells, but not in FSHR-re-directed CERT cells in this particular case. Because all signaling motifs were identical in both formulations, these data strongly suggest that tumor ascites elicits specific activation of CAR T cells in an antigen-specific manner. Taken together, these results indicate that chimeric receptor-targeted T-cells persist as memory cells in treated ovarian cancer-bearing hosts, but in the presence of advanced tumor ascites, they eventually disappear from tumor beds. Release of continuously expressed molecular target into ascites in exosomes activates T-cells distally from tumor cells, thus impairing therapeutic effectiveness, despite apparent lack of exhaustion and persistence in lymphoid organs.

## DISCUSSION

Here we showed that T-cells re-directed with FSHR-targeted chimeric receptors attack ovarian cancer cells and mediate significant therapeutic effects, including tumor rejection against different established patient-derived tumors.

Our study identifies FSHR as an immunotherapeutic target expressed not only by serous ovarian carcinomas, but also by other particularly aggressive and chemoresistant histological types, such as clear cell and mucinous tumors. Most importantly, we did not detect expression of FSHR in any healthy tissue with the exception of ovaries. Accordingly, mouse T-cells redirected with murine FSH to target syngeneic tumors did not induce any detectable alteration in liver, kidney, or endocrine pancreatic function. Other authors have recently shown that FSH hormone fragments can delay the *in vivo* growth of established cell lines (42). Although FSH $\beta$  alone was not effective in our hands, the use of the two subunits of FSH rendered T cells effective against different patient-derived tumors expressing variable levels of FSHR. Therefore, FSHR, and perhaps other hormone receptors with a very restricted expression pattern in other tumors represent promising targets to translate the success of CAR T-cells from hematologic to solid tumors without fatal off-target effects. Furthermore, the natural affinity of FSH for its endogenous receptor not only ensures maximum specificity, but should also prevent immunological rejection of the chimeric receptor, which is a concern for constructs using exogenous antibody fragments.

Our work also demonstrates for the first time that host-derived T-cells influenced by chimeric receptor-transduced lymphocytes could contribute to overall effectiveness. Accordingly, recent studies showed that short-lived mesothelin-targeting CAR T-cells can induce epitope-spreading and raise Ab titers in patients (41). Our work in immunocompetent preclinical models expands these mechanisms by demonstrating that FSHRCER T-cells increase endogenous T-cell activity, which is sufficient to delay tumor progression. These effects may be particularly important in tumors undergoing loss of targeted antigens through immunoediting or deletion of CAR T-cells because polyclonal responses could provide immune pressure against malignant progression even after transferred lymphocytes become ineffective. Of note, we also observed a measurable boost in pre-existing anti-tumor immunity upon transferring mock-transduced T-cells versus the PBS treated group. This is in line with our previously reported immunogenic boost upon adoptive transfer of unstimulated T cells (7), and likely reflects a change in the cytokine milieu in response to adoptive T cell transfer. However, we did not observe any loss of antigenicity in our systems at end-stage disease, although FSHR-targeted chimeric receptor-expressing T-cells remained in the host until tumor-bearing mice succumbed to terminal disease. However, release of targeted molecules from the surface of tumor cells in ascites could divert the effector activity of chimeric receptor-expressing T-cells away from tumor cells. Patients with reduced ascites burden or administration of FSHRCER T-cells between initial treatment and recurrence would therefore be preferable to maximize effectiveness.

Overall, our study demonstrates the effectiveness and safety of targeting chimeric receptors for T-cell activation using full-length hormones and unveils mechanisms of therapeutic activity that contribute to understanding the effects of adoptively transferred T-cells in ongoing and future clinical trials.

## Supplementary Material

Refer to Web version on PubMed Central for supplementary material.

## ACKNOWLEDGEMENTS

Support for Shared Resources was provided by Cancer Center Support Grant (CCSG) CA010815 to The Wistar Institute. We are grateful to the Flow Cytometry Facility at Wistar for outstanding insight.

**FINANCIAL SUPPORT:** JRCG: R01CA157664, R01CA124515, R01CA178687, P30CA10815, The Jayne Koskinas & Ted Giovanis Breast Cancer Research Consortium at Wistar and Ovarian Cancer Research Fund Program Project Development awards. MJA and NS were supported by T32CA009171. KKP was supported by was supported by T32CA009140. APP was supported by the Ann Schreiber Mentored Investigator Award (OCRF).

## REFERENCES

1. Jemal A, Siegel R, Ward E, Hao Y, Xu J, Thun MJ. Cancer statistics, 2009. *CA Cancer J Clin.* 2009; 59:225–49. [PubMed: 19474385]
2. Curiel TJ, Coukos G, Zou L, Alvarez X, Cheng P, Mottram P, et al. Specific recruitment of regulatory T cells in ovarian carcinoma fosters immune privilege and predicts reduced survival. *Nat Med.* 2004; 10:942–9. [PubMed: 15322536]
3. Zhang L, Conejo-Garcia JR, Katsaros D, Gimotty PA, Massobrio M, Regnani G, et al. Intratumoral T cells, recurrence, and survival in epithelial ovarian cancer. *N Engl J Med.* 2003; 348:203–13. [PubMed: 12529460]

4. Cubillos-Ruiz JR, Engle X, Scarlett UK, Martinez D, Barber A, Elgueta R, et al. Polyethylenimine-based siRNA nanocomplexes reprogram tumor-associated dendritic cells via TLR5 to elicit therapeutic antitumor immunity. *J Clin Invest*. 2009; 119:2231–44. [PubMed: 19620771]
5. Cubillos-Ruiz JR, Martinez D, Scarlett UK, Rutkowski MR, Nesbeth YC, Camposeco-Jacobs AL, et al. CD277 is a Negative Co-stimulatory Molecule Universally Expressed by Ovarian Cancer Microenvironmental Cells. *Oncotarget*. 2010; 1:329–8. [PubMed: 21113407]
6. Huarte E, Cubillos-Ruiz JR, Nesbeth YC, Scarlett UK, Martinez DG, Buckanovich RJ, et al. Depletion of dendritic cells delays ovarian cancer progression by boosting antitumor immunity. *Cancer Res*. 2008; 68:7684–91. [PubMed: 18768667]
7. Nesbeth Y, Scarlett U, Cubillos-Ruiz J, Martinez D, Engle X, Turk MJ, et al. CCL5-mediated endogenous antitumor immunity elicited by adoptively transferred lymphocytes and dendritic cell depletion. *Cancer Res*. 2009; 69:6331–8. [PubMed: 19602595]
8. Scarlett UK, Cubillos-Ruiz JR, Nesbeth YC, Martinez DG, Engle X, Gewirtz AT, et al. In situ stimulation of CD40 and Toll-like receptor 3 transforms ovarian cancer-infiltrating dendritic cells from immunosuppressive to immunostimulatory cells. *Cancer Res*. 2009; 69:7329–37. [PubMed: 19738057]
9. Scarlett UK, Rutkowski MR, Rauwerdink AM, Fields J, Escovar-Fadul X, Baird J, et al. Ovarian cancer progression is controlled by phenotypic changes in dendritic cells. *J Exp Med*. 2012; 209:495–506. [PubMed: 22351930]
10. Cubillos-Ruiz JR, Baird JR, Tesone AJ, Rutkowski MR, Scarlett UK, Camposeco-Jacobs AL, et al. Reprogramming tumor-associated dendritic cells in vivo using microRNA mimetics triggers protective immunity against ovarian cancer. *Cancer Res*. 2012; 72:1683–93. [PubMed: 22307839]
11. Brayer JB, Pinilla-Ibarz J. Developing strategies in the immunotherapy of leukemias. *Cancer Control*. 2013; 20:49–59. [PubMed: 23302907]
12. Nelson MH, Paulos CM. Novel immunotherapies for hematologic malignancies. *Immunol Rev*. 2015; 263:90–105. [PubMed: 25510273]
13. Porter DL, Levine BL, Kalos M, Bagg A, June CH. Chimeric antigen receptor-modified T cells in chronic lymphoid leukemia. *N Engl J Med*. 2011; 365:725–33. [PubMed: 21830940]
14. Maus MV, Grupp SA, Porter DL, June CH. Antibody-modified T cells: CARs take the front seat for hematologic malignancies. *Blood*. 2014; 123:2625–35. [PubMed: 24578504]
15. Kalos M, Levine BL, Porter DL, Katz S, Grupp SA, Bagg A, et al. T cells with chimeric antigen receptors have potent antitumor effects and can establish memory in patients with advanced leukemia. *Sci Transl Med*. 2011; 3:95ra73.
16. Simoni M, Gromoll J, Nieschlag E. The follicle-stimulating hormone receptor: biochemistry, molecular biology, physiology, and pathophysiology. *Endocr Rev*. 1997; 18:739–73. [PubMed: 9408742]
17. Vannier B, Loosfelt H, Meduri G, Pichon C, Milgrom E. Anti-human FSH receptor monoclonal antibodies: immunochemical and immunocytochemical characterization of the receptor. *Biochemistry*. 1996; 35:1358–66. [PubMed: 8634264]
18. Zhang XY, Chen J, Zheng YF, Gao XL, Kang Y, Liu JC, et al. Follicle-stimulating hormone peptide can facilitate paclitaxel nanoparticles to target ovarian carcinoma in vivo. *Cancer Res*. 2009; 69:6506–14. [PubMed: 19638590]
19. Al-Timimi A, Buckley CH, Fox H. An immunohistochemical study of the incidence and significance of human gonadotrophin and prolactin binding sites in normal and neoplastic human ovarian tissue. *Br J Cancer*. 1986; 53:321–9. [PubMed: 3083857]
20. Zhang X, Chen J, Kang Y, Hong S, Zheng Y, Sun H, et al. Targeted paclitaxel nanoparticles modified with follicle-stimulating hormone beta 81-95 peptide show effective antitumor activity against ovarian carcinoma. *Int J Pharm*. 2013; 453:498–505. [PubMed: 23811008]
21. Minegishi T, Kameda T, Hirakawa T, Abe K, Tano M, Ibuki Y. Expression of gonadotropin and activin receptor messenger ribonucleic acid in human ovarian epithelial neoplasms. *Clin Cancer Res*. 2000; 6:2764–70. [PubMed: 10914722]
22. Nakano R, Kitayama S, Yamoto M, Shima K, Ooshima A. Localization of gonadotropin binding sites in human ovarian neoplasms. *Am J Obstet Gynecol*. 1989; 161:905–10. [PubMed: 2552807]

23. Parrott JA, Doraiswamy V, Kim G, Mosher R, Skinner MK. Expression and actions of both the follicle stimulating hormone receptor and the luteinizing hormone receptor in normal ovarian surface epithelium and ovarian cancer. *Mol Cell Endocrinol.* 2001; 172:213–22. [PubMed: 11165055]
24. Wang J, Lin L, Parkash V, Schwartz PE, Lauchlan SC, Zheng W. Quantitative analysis of follicle-stimulating hormone receptor in ovarian epithelial tumors: a novel approach to explain the field effect of ovarian cancer development in secondary mullerian systems. *Int J Cancer.* 2003; 103:328–34. [PubMed: 12471615]
25. Zheng W, Lu JJ, Luo F, Zheng Y, Feng Y, Felix JC, et al. Ovarian epithelial tumor growth promotion by follicle-stimulating hormone and inhibition of the effect by luteinizing hormone. *Gynecol Oncol.* 2000; 76:80–8. [PubMed: 10620446]
26. Chen FC, Oskay-Ozcelik G, Buhling KJ, Kopstein U, Mentze M, Lichtenegger W, et al. Prognostic value of serum and ascites levels of estradiol, FSH, LH and prolactin in ovarian cancer. *Anticancer Res.* 2009; 29:1575–8. [PubMed: 19443368]
27. Conejo-Garcia JR, Benencia F, Courreges MC, Kang E, Mohamed-Hadley A, Buckanovich RJ, et al. Tumor-infiltrating dendritic cell precursors recruited by a beta-defensin contribute to vasculogenesis under the influence of Vegf-A. *Nat Med.* 2004; 10:950–8. [PubMed: 15334073]
28. Rutkowski MR, Allegrezza MJ, Svoronos N, Tesone AJ, Stephen TL, Perales-Puchalt A, et al. Initiation of metastatic breast carcinoma by targeting of the ductal epithelium with adenovirus-cre: a novel transgenic mouse model of breast cancer. *J Vis Exp.* 2014
29. Rutkowski MR, Stephen TL, Svoronos N, Allegrezza MJ, Tesone AJ, Perales-Puchalt A, et al. Microbially driven TLR5-dependent signaling governs distal malignant progression through tumor-promoting inflammation. *Cancer Cell.* 2015; 27:27–40. [PubMed: 25533336]
30. Ozdemir O, Ravindranath Y, Savasan S. Cell-mediated cytotoxicity evaluation using monoclonal antibody staining for target or effector cells with annexinV/propidium iodide colabeling by fluorosphere-adjusted counts on three-color flow cytometry. *Cytometry A.* 2003; 56:53–60. [PubMed: 14566939]
31. Radu A, Pichon C, Camparo P, Antoine M, Allory Y, Couvelard A, et al. Expression of follicle-stimulating hormone receptor in tumor blood vessels. *N Engl J Med.* 2010; 363:1621–30. [PubMed: 20961245]
32. McCluggage WG. Morphological subtypes of ovarian carcinoma: a review with emphasis on new developments and pathogenesis. *Pathology.* 2011; 43:420–32. [PubMed: 21716157]
33. Katsumata N, Yasuda M, Isonishi S, Takahashi F, Michimae H, Kimura E, et al. Long-term results of dose-dense paclitaxel and carboplatin versus conventional paclitaxel and carboplatin for treatment of advanced epithelial ovarian, fallopian tube, or primary peritoneal cancer (JGOG 3016): a randomised, controlled, open-label trial. *Lancet Oncol.* 2013; 14:1020–6. [PubMed: 23948349]
34. Choi JH, Choi KC, Auersperg N, Leung PC. Overexpression of follicle-stimulating hormone receptor activates oncogenic pathways in preneoplastic ovarian surface epithelial cells. *J Clin Endocrinol Metab.* 2004; 89:5508–16. [PubMed: 15531506]
35. Song Y, Wang ES, Xing LL, Shi S, Qu F, Zhang D, et al. Follicle-Stimulating Hormone Induces Postmenopausal Dyslipidemia Through Inhibiting Hepatic Cholesterol Metabolism. *J Clin Endocrinol Metab.* 2016; 101:254–63. [PubMed: 26583582]
36. Stephen TL, Rutkowski MR, Allegrezza MJ, Perales-Puchalt A, Tesone AJ, Svoronos N, et al. Transforming Growth Factor beta-Mediated Suppression of Antitumor T Cells Requires FoxP1 Transcription Factor Expression. *Immunity.* 2014; 41:427–39. [PubMed: 25238097]
37. Nesbeth YC, Martinez DG, Toraya S, Scarlett UK, Cubillos-Ruiz JR, Rutkowski MR, et al. CD4+ T cells elicit host immune responses to MHC class II- ovarian cancer through CCL5 secretion and CD40-mediated licensing of dendritic cells. *J Immunol.* 2010; 184:5654–62. [PubMed: 20400704]
38. Rutkowski MR, Conejo-Garcia JR. TLR5 signaling, commensal microbiota and systemic tumor promoting inflammation: the three parcae of malignant progression. *Oncoimmunology.* 2015; 4:e1021542. [PubMed: 26405577]

39. Grupp SA, Kalos M, Barrett D, Aplenc R, Porter DL, Rheingold SR, et al. Chimeric antigen receptor-modified T cells for acute lymphoid leukemia. *N Engl J Med.* 2013; 368:1509–18. [PubMed: 23527958]
40. Siraj A, Desestret V, Antoine M, Fromont G, Huerre M, Sanson M, et al. Expression of follicle-stimulating hormone receptor by the vascular endothelium in tumor metastases. *BMC Cancer.* 2013; 13:246. [PubMed: 23688201]
41. Beatty GL, Haas AR, Maus MV, Torigian DA, Soulen MC, Plesa G, et al. Mesothelin-specific chimeric antigen receptor mRNA-engineered T cells induce anti-tumor activity in solid malignancies. *Cancer Immunol Res.* 2014; 2:112–20. [PubMed: 24579088]
42. Urbanska K, Stashwick C, Poussin M, Powell DJ Jr. Follicle-Stimulating Hormone Receptor as a Target in the Redirected T-cell Therapy for Cancer. *Cancer Immunol Res.* 2015; 3:1130–7. [PubMed: 26112923]

**STATEMENT OF CLINICAL RELEVANCE**

The outcome of ovarian cancer patients has improved very little over the last 40 years. As an immunogenic disease, immunotherapies targeting epithelial ovarian cancer offer great hope to reverse this dismaying prognosis. We show that follicle-stimulating hormone (FSH) receptor is expressed on the cell surface of ovarian carcinomas of different histological types, including clear cell and mucinous tumors, which are particularly aggressive. Most importantly, no FSHR expression is found in non-ovarian healthy tissues in adult women. Accordingly, T-cells expressing full-length FSHR-re-directed chimeric receptors mediate significant therapeutic effects (including tumor rejection) against established patient-derived and transplantable tumors *in vivo*, without any measurable toxicity in immunocompetent mice treated with T-cells targeting murine FSHR. Therefore, T-cells redirected against FSHR<sup>+</sup> tumor cells with full-length FSH represent a promising therapeutic alternative against a broad range of ovarian malignancies, with negligible toxicity even in the presence of cognate targets in tumor-free ovaries.

Author Manuscript

Author Manuscript

Author Manuscript

Author Manuscript



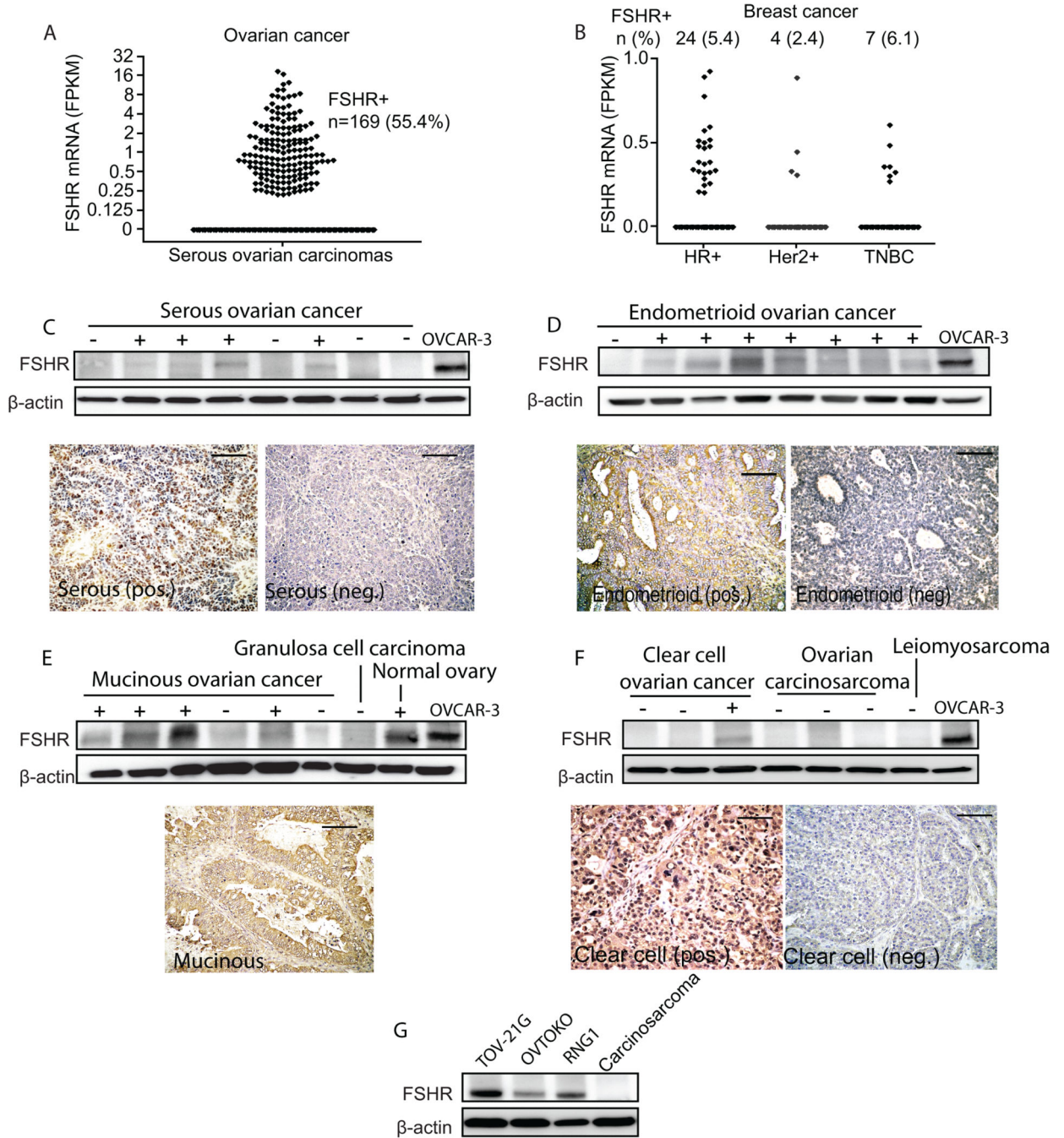


**Figure 1. FSHR is expressed in aggressive ovarian carcinomas of multiple histological subtypes** (A) Scatter plot of the level of FSHR mRNA from 404 cases of serous ovarian cancer from TCGA dataset (measured as FKPM) with number (n) and percentage (%) of FSHR expressing tumors (B) Scatter plot of the level of FSHR mRNA from 1095 cases of breast cancer from TCGA dataset divided as hormone receptor positive (HR+), Her2/Neu positive (Her+) and triple negative breast cancer (TNBC), with number (n) and percentage (%) of FSHR expressing tumors. Western blot and immunohistochemistry (20x) showing expression of FSHR in randomly selected ovarian (C) serous, (D) endometrioid, (E)

mucinous, granulosa cell, (F) clear cell and carcinosarcoma tumors from our tumor bank. We used the OVCAR-3 ovarian cancer cell line as positive control. Scale bar, 100  $\mu\text{m}$ . (G) Western blot showing expression of FSHR in ovarian clear cell carcinoma cell lines TOV-21G, RNG1 and OVTOKO. A carcinosarcoma sample was used as negative control.

Author Manuscript

Author Manuscript

Author Manuscript

Author Manuscript

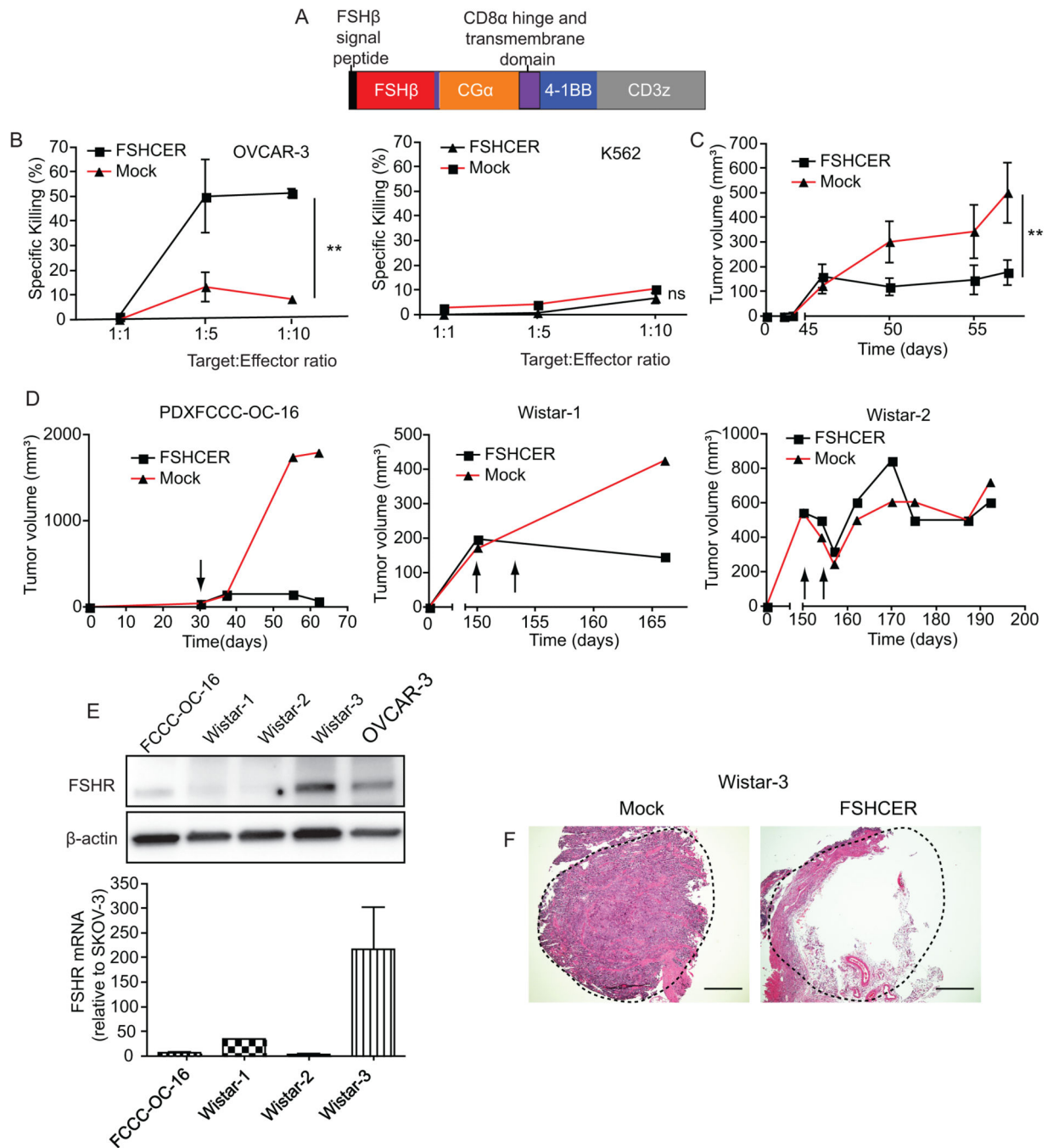


**Figure 2. FSHR can be effectively targeted to treat ovarian cancer through the use of chimeric antigen receptors**  
**(A)** Schematic of FSHCER **(B)** Cytotoxicity of FSHCER or mock transduced T-cells of OVCAR-3 and K562 measured by 7-AAD/Annexin V flow cytometric staining after co-culture of 18 hours. **(C)** Tumor volume of CaOV3 cell line grown in the flank of NOD-SCID mice (n=4 per group; single experiment) after treatment with a single intra-tumoral injection of 6 million FSHCER or mock transduced T cells when tumor mean volume was approximately 150mm<sup>3</sup>. **(D)** Tumor volume of three ovarian patient-derived xenograft

tumors grown in the flank of NOD-SCID mice (n=2 mice per tumor, one case-one control, single experiment) injected intratumorally with 10 million FSHCER or mock transduced T-cells (arrows mark time of T-cell injection). **(E)** Western blot and qPCR showing FSHR expression of treated ovarian PDX tumors. OVCAR-3 is shown as positive control. **(F)** Hematoxylin-Eosin staining of ovarian PDX tumor grown in NOD-SCID mice ovary treated with either FSHCER or mock transduced autologous T-cells. \*p<0.05, \*\*p 0.01, \*\*\*p 0.001, ns: not significant.

Author Manuscript

Author Manuscript

Author Manuscript

Author Manuscript

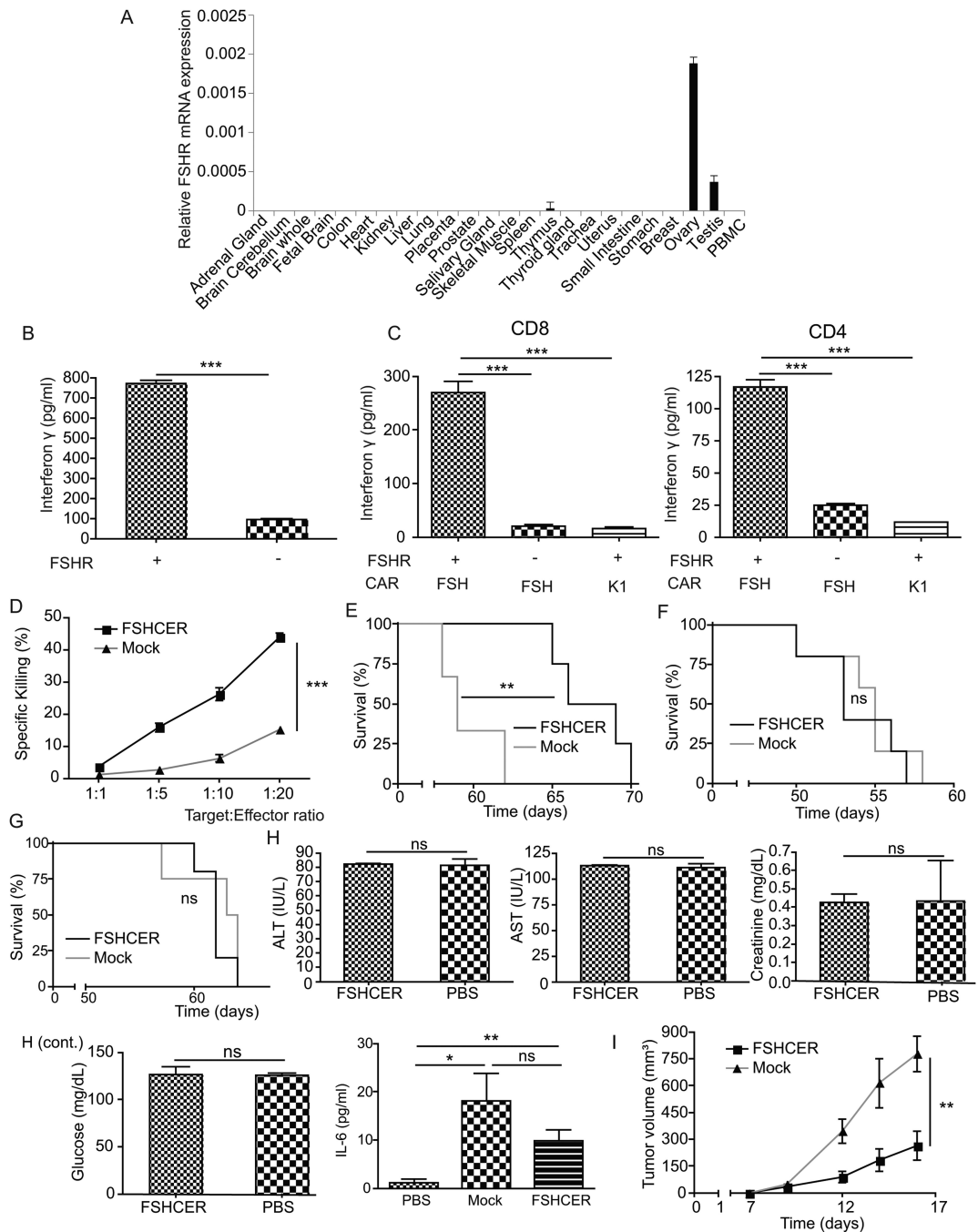


**Figure 3. Chimeric-receptor-expressing T-cells delay malignant progression in immunocompetent cancer bearing mice**

(A) Normalized real-time quantitative-PCR of FSHR expression in human healthy tissues. (B) Levels of interferon- $\gamma$  in supernatants from coculture of ID8-*Defb29/Vegf-a/Fshr* or ID8-*Defb29/Vegf-a* with FSHCER or K1CAR transduced T-cells by ELISA. (C) Levels of interferon  $\gamma$  in supernatants from co-culture of ID8-*Defb29/Vegf-a-Fshr* or ID8-*Defb29/Vegf-a* with FSHCER or K1CAR (irrelevant anti-mesothelin CAR) transduced CD4 or CD8 T-cells by ELISA (D) Cytotoxicity of FSHCER or mock transduced T-cells of ID8-*Defb29/Vegf-a*

*Vegf-a/Fshr* measured by 7-AAD/Annexin V staining after co-culture of 18 hours. **(E)** Survival plot of mice bearing intraperitoneal ID8-*Defb29/Vegf-a/Fshr* syngeneic tumors treated intraperitoneally with FSHCER or mock transduced T-cells at days 7 and 14 after tumor challenge (n=5 per group; 3 independent experiments). **(F)** Survival plot of mice bearing intraperitoneal ID8-*Defb29/Vegf-a/Fshr* syngeneic tumors treated intravenously with 1.5 million FSHCER or mock transduced T-cells at days 7 and 14 after tumor challenge (n=5 per group; 1 independent experiment). **(G)** Survival plot of mice bearing intraperitoneal ID8-*Defb29/Vegf-a* syngeneic tumors treated intraperitoneally with 1.5 million FSHCER or mock transduced T-cells at days 7 and 21 after tumor challenge (n=5 per group; 1 independent experiment). **(H)** Determination in FSHCER versus PBS treated mice of serum AST, ALT, creatinine, glucose and IL-6 (n=4 per group; single experiment). **(I)** Growth kinetics of A7C11 flank tumors expressing FSHR treated intraperitoneally with FSHCER or mock transduced T-cells at days 7 and 14 after tumor challenge (n=5 per group; 3 independent experiments). ns: not significant, \*p<0.05, \*\*p 0.01, \*\*\*p 0.001

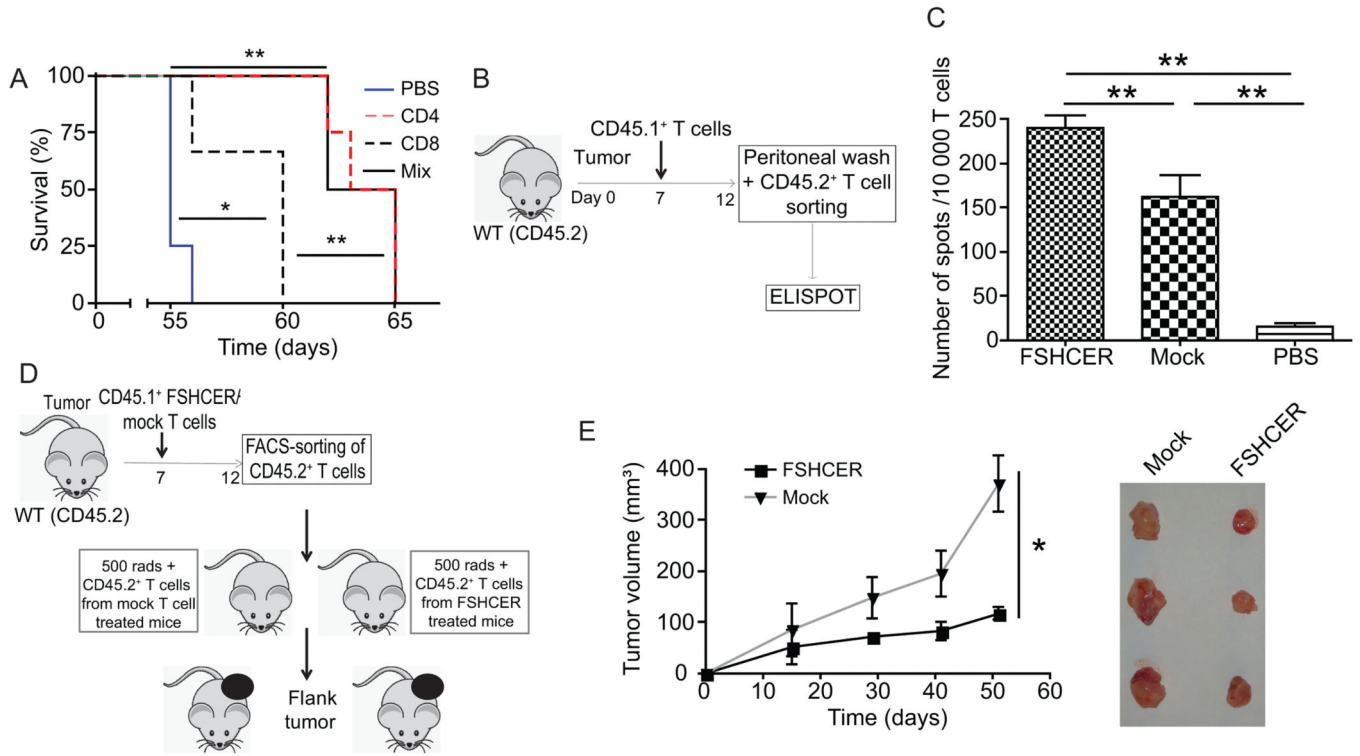


**Figure 4. Chimeric receptor-expressing T-cells boost pre-existing (endogenous) T-cell-dependent anti-tumor immunity**

(A) Survival plot of mice bearing ID8-*Defb29/Vegf-a/Fshr* ovarian tumors treated with either CD4, CD8, or a mixed population of T-cells bearing the FSHCER (n=4 per group; single experiment). (B) Experiment schematic: CD45.2<sup>+</sup> mice bearing ID8-*Defb29/Vegf-a/Fshr* syngeneic tumors were treated with either CAR T-cells (1.5e<sup>6</sup> CD45.1<sup>+</sup> cells intraperitoneally), mock-transduced T-cells (1.5e<sup>6</sup> CD45.1<sup>+</sup> cells intraperitoneally) or PBS. One week later we FACS-sorted endogenous (CD45.2<sup>+</sup>GFP<sup>-</sup>) T-cells from ascites and analyzed their antitumor activity using interferon-gamma ELISPOT. (C) Interferon-gamma ELISPOT of endogenous CD45.2 T-cells derived from ascites of FSHCER or PBS treated mice, primed with ID8-*Defb29/Vegf-a/Fshr* pulsed DCs (n=2-4 per group). (D) Experiment schematic: CD45.2<sup>+</sup> mice bearing ID8-*Defb29/Vegf-a/Fshr* ovarian tumors were treated with either FSHCER or mock transduced T-cells (1.5e<sup>6</sup> CD45.1<sup>+</sup> cells intraperitoneally). One week later we FACS-sorted endogenous (CD45.2<sup>+</sup>GFP<sup>-</sup>) T-cells from the spleen and injected one million per mouse to sublethally irradiated mice. One day later we injected these mice in the flank with ID8-*Defb29/Vegf-a/Fshr*. (E) Tumor volumes and tumors after resection of ID8-*Defb29/Vegf-a/Fshr* flank tumors treated with endogenous (1e<sup>6</sup> CD45.2<sup>+</sup>GFP<sup>-</sup> cells administered intraperitoneally) T-cells (n=4-5 per group; 2 independent experiments). Tumors from an individual experiment are depicted. \*p<0.05, \*\*p 0.01, \*\*\*p 0.001

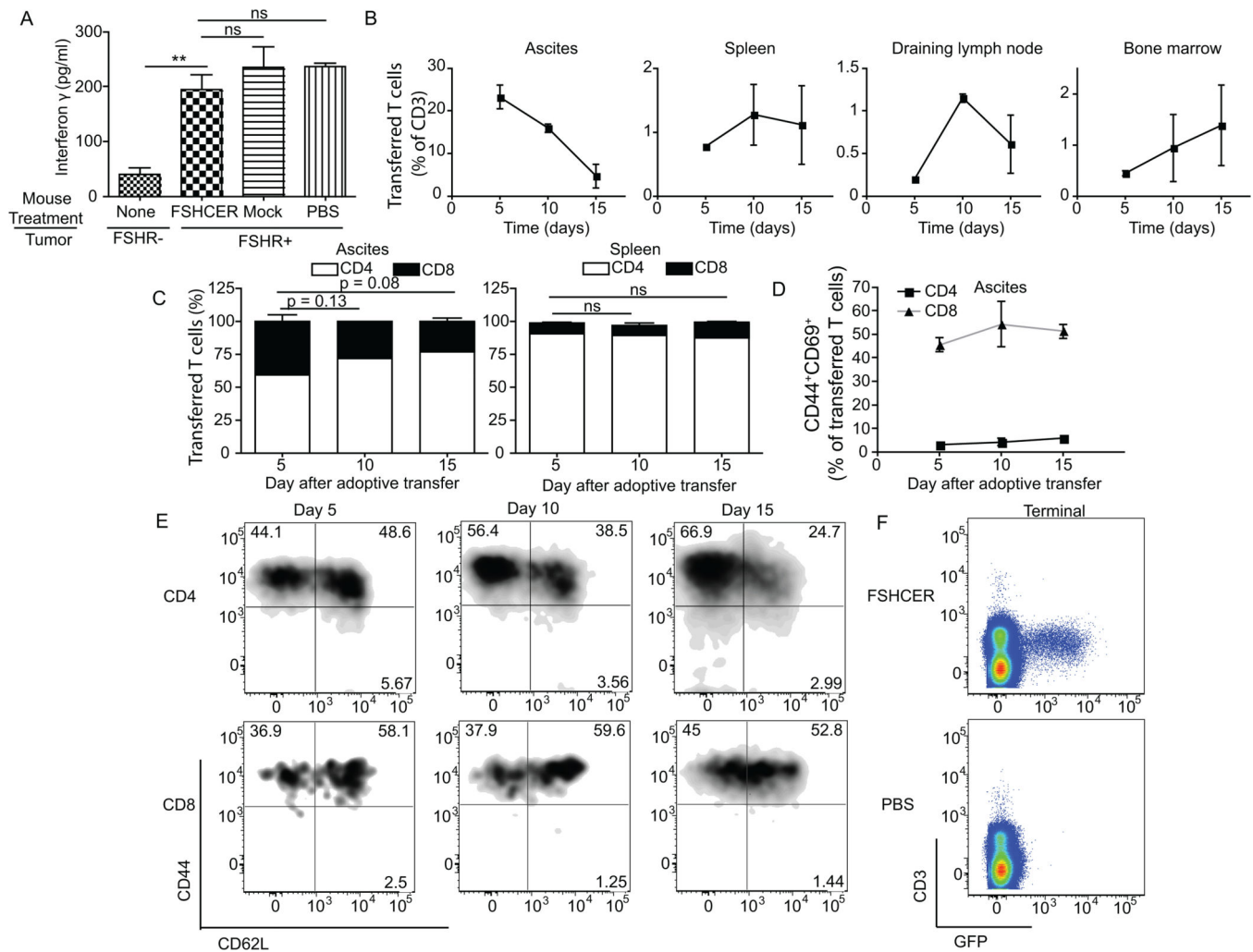


**Figure 5. Chimeric receptor-expressing T-cells persist in the absence of immunoeediting**  
**(A)** Levels of interferon- $\gamma$  elicited by fresh FSHCER- or mock-transduced T-cells after incubation of ID8-*Defb29/Vegf-a/Fshr* cells (1:10 target:effector ratio), FACS-sorted from the peritoneal cavity of orthotopic ID8-*Defb29/Vegf-a/Fshr*-bearing mice treated with either FSHCER, mock transduced T-cells or PBS. **(B)** Percentage of transferred CAR T-cells (CD45.1<sup>+</sup>GFP<sup>+</sup>) out of CD45<sup>+</sup>CD3<sup>+</sup> T-cells in the peritoneal cavity, spleen, draining lymph node and bone marrow of ID8-*Defb29/Vegf-a/Fshr* orthotopic ovarian tumors, at days 5, 10 and 15 after treatment. **(C)** Percentage of CD4 and CD8 in peritoneal cavity and spleen at days 5, 10 and 15 after treatment. **(D)** Percentage of activated transferred T-cells (CD45.1<sup>+</sup>GFP<sup>+</sup>CD44<sup>+</sup>CD69<sup>+</sup>) in the peritoneal cavity of ID8-*Defb29/Vegf-a/Fshr* orthotopic ovarian tumors, at days 5, 10 and 15 after treatment (n=2 per group; 4 independent experiments). **(E)** Percentage of naïve, central memory and effector memory transferred T-cells (CD45.1<sup>+</sup>GFP<sup>+</sup>) in the peritoneal cavity of ID8-*Defb29/Vegf-a/Fshr* orthotopic ovarian tumors, at days 5, 10 and 15 after treatment (n=2 per group; 4 independent experiments). **(F)** FSHCER T-cells (GFP<sup>+</sup>) in the spleen of FSHCER and vehicle (PBS) treated mice bearing ID8-*Defb29/Vegf-a/Fshr* orthotopic tumors, at the time of terminal ascites, gated out of CD45<sup>+</sup>. ns: not significant, \*p<0.05, \*\*p 0.01, \*\*\*p 0.001.



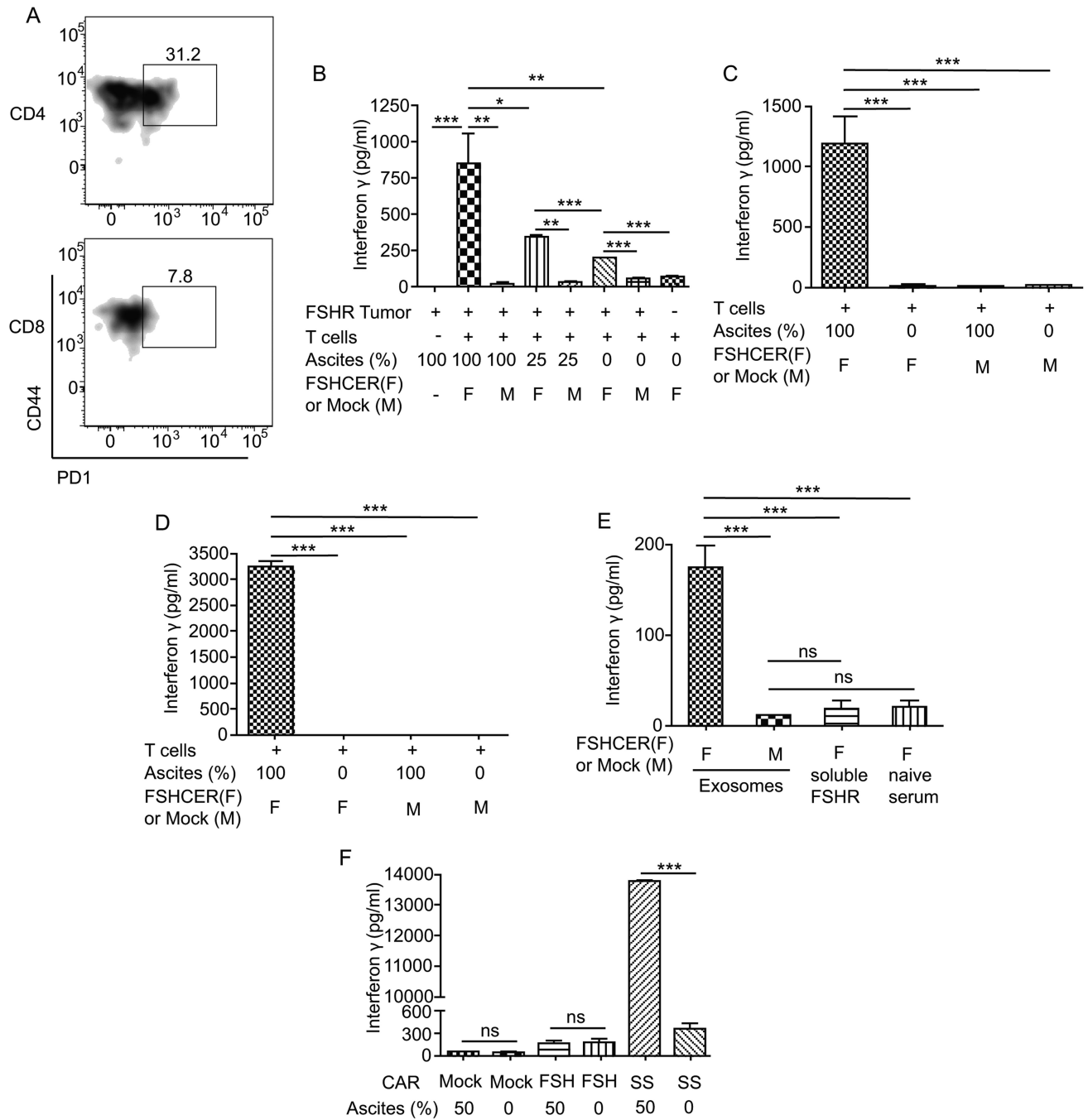


**Figure 6. Exosomes in FSHR<sup>+</sup> tumor ascites elicit T cell activation distally from tumor cells**  
**(A)** Percentage of transferred CD4 and CD8 T-cells in the spleen expressing PD-1 at the time of terminal ascites. **(B)** Levels of interferon gamma elicited after incubation of ID8-*Defb29/Vegfa/Fshr* cells (1:10 target:effector ratio) with either FSHCER or mock transduced T-cells with the indicated percentages of cell-free ascites from ID8-*Defb29/Vegfa/Fshr* bearing mice. **(C)** Levels of interferon gamma elicited after incubation of ID8-*Defb29/Vegfa/Fshr* cells (1:10 target:effector ratio) with either FSHCER or mock transduced T-cells with the indicated percentages of cell free ascites from ID8-*Defb29/Vegfa/Fshr*-bearing mice

Author Manuscript

Author Manuscript

Author Manuscript

Author Manuscript

using a transwell plate with 0.4um pore size to avoid T cell-tumor cell contact. **(D)** Levels of interferon gamma elicited after FSHCER or mock transduced T-cells with the cell-free ascites from ID8-*Defb29/Vegf-a/Fshr* bearing mice or RPMI-10%FBS in the absence target cells. **(E)** Levels of interferon gamma elicited after incubation of ascites derived-exosomes from mice bearing ID8-*Defb29/Vegf-a/Fshr* tumors, soluble mouse FSHR and plasma from naïve mice with either FSHCER or mock transduced T-cells. **(F)** Levels of IFN- $\gamma$  elicited after SSCAR, FSHCER or mock transduced T-cells with cell-free ascites from an ovarian cancer patient or RPMI-10%FBS. \* $p < 0.05$ , \*\* $p < 0.01$ , \*\*\* $p < 0.001$ , ns: not significant.